BDNF is a mediator of glycolytic fiber-type specification in mouse skeletal muscle

Julien Delezie[a], Martin Weihrauch[a], Geraldine Maier[a], Rocío Tejero[b], Daniel J. Ham[a], Jonathan F. Gill[a], Bettina Karrer-Cardel[a], Markus A. Rüegg[a], Lucía Tabares[b], and Christoph Handschin[a,1]

[a]Biozentrum, University of Basel, CH-4056 Basel, Switzerland; and [b]Department of Medical Physiology and Biophysics, School of Medicine, University of Seville, 41009 Seville, Spain

Edited by Louis M. Kunkel, Boston Children's Hospital, Harvard Medical School, Boston, MA, and approved June 24, 2019 (received for review January 11, 2019)

Brain-derived neurotrophic factor (BDNF) influences the differentiation, plasticity, and survival of central neurons and likewise, affects the development of the neuromuscular system. Besides its neuronal origin, BDNF is also a member of the myokine family. However, the role of skeletal muscle-derived BDNF in regulating neuromuscular physiology in vivo remains unclear. Using gain- and loss-of-function animal models, we show that muscle-specific ablation of BDNF shifts the proportion of muscle fibers from type IIB to IIX, concomitant with elevated slow muscle-type gene expression. Furthermore, BDNF deletion reduces motor end plate volume without affecting neuromuscular junction (NMJ) integrity. These morphological changes are associated with slow muscle function and a greater resistance to contraction-induced fatigue. Conversely, BDNF overexpression promotes a fast muscle-type gene program and elevates glycolytic fiber number. These findings indicate that BDNF is required for fiber-type specification and provide insights into its potential modulation as a therapeutic target in muscle diseases.

neurotrophic factor | myokine | oxidative fiber | neuromuscular junction | endurance exercise

Neurotrophins (NTs) are members of a subfamily of structurally related trophic factors that regulate the differentiation, survival, and function of neuronal cells by modulating the $p75^{NTR}$ receptor and members of the Trk family of receptor tyrosine kinases (1, 2). Besides the central nervous system, skeletal muscle is an abundant source of trophic factors during development (3, 4). In particular, NTs can be released from muscle fibers, acting on the nerve terminals of motor neurons (5, 6), in addition to using retrograde routes to be transported to the cell body (7, 8).

Inactivation or overexpression of NTs in mouse models demonstrates their broad involvement in neuromuscular physiology. For instance, chronic deprivation of the nerve growth factor leads to muscular dystrophy (9). Deficiency in NT-3 or its receptor TrkC decreases proprioceptive afferents and muscle spindles, resulting in severe movement defects (10, 11). Lack of NT-4/5 induces the disassembly of postsynaptic acetylcholine receptor (AChR) clusters in association with neurotransmission failure and decreased fatigue resistance (12).

Similar to these NT family members, the brain-derived neurotrophic factor (BDNF) also exerts diverse roles in the neuromuscular system. For example, BDNF regulates agrin-induced AChR clustering in cultured myotubes (13). Moreover, precursor and mature forms of BDNF influence the survival and innervation pattern of developing motor neurons by modulating both $p75^{NTR}$ and TrkB receptors (8, 14). Accordingly, mice heterozygous for TrkB display altered neuromuscular junction (NMJ) structure and function as well as muscle weakness and sarcopenia (6, 15). In contrast to BDNF of neuronal origin, the role of BDNF in muscle function is much less studied, in part due to controversial BDNF detection in this tissue (16). There is, however, evidence that BDNF is a contraction-induced myokine likely involved in autocrine and/or paracrine regulation of muscle fat metabolism (17). Moreover, specific loss of BDNF within the satellite cell niche affects early stages of the regenerative process after muscle cardiotoxin injury (18). However, no study to date has comprehensively investigated the potential contribution of skeletal muscle-derived BDNF to both muscle and NMJ physiology in the postnatal mouse in vivo.

Using functional, cellular, and molecular approaches, we show that mice lacking BDNF specifically in striated muscle fibers do not exhibit any developmental neuromuscular or metabolic deficits. Intriguingly, we discovered that loss of BDNF within muscle fibers induces structural and functional remodeling of the NMJ toward a slower phenotype. In line, our data indicate that muscle BDNF loss or gain of function is sufficient to decrease or increase, respectively, the proportion of types IIB and IIX muscle fibers along with a broad range of oxidative and glycolytic marker genes.

Results

BDNF Muscle Knockout Mice Show Altered Spontaneous Gait Behavior and Locomotion. To restrict the Cre-induced recombination of the *Bdnf* floxed allele to skeletal muscle cells, we used the human α-skeletal actin (HSA) promoter (19, 20). $Bdnf^{flox/flox}$;HSA-Cre mice (hereafter referred as muscle knockout [MKO]) were born at Mendelian ratios and exhibited an average lifespan comparable with their $Bdnf^{flox/flox}$ control (CTRL) littermates (CTRL: 833.1 ± 38.2 d vs. MKO: 880 ± 31.3 d; $n = 10$ per genotype; not significant).

Significance

The brain-derived neurotrophic factor (BDNF) is essential to promote neuronal differentiation, plasticity, and survival. Altered BDNF expression is associated with several pathologies, including neuropsychiatric and neurodegenerative disorders, cardiovascular diseases, diabetes, and motor neuron diseases. Although BDNF has been identified as a contraction-induced myokine, its involvement in muscle physiology is unclear. Using functional, cellular, and molecular approaches, we report here that the myokine BDNF regulates glycolytic muscle fiber-type identity. Our findings warrant additional studies to determine whether modulating the activity of BDNF represents an effective therapeutic strategy to delay or even prevent muscle wasting disorders in which the function of glycolytic muscle fibers is compromised (e.g., in Duchenne muscular dystrophy, muscle insulin resistance).

Author contributions: J.D. and C.H. designed research; J.D., M.W., G.M., R.T., D.J.H., J.F.G., and B.K.-C. performed research; M.A.R. and L.T. contributed new reagents/analytic tools; J.D., R.T., and D.J.H. analyzed data; and J.D. and C.H. wrote the paper.

The authors declare no conflict of interest.

This article is a PNAS Direct Submission.

[1]To whom correspondence may be addressed. Email: christoph.handschin@unibas.ch.

This article contains supporting information online at www.pnas.org/lookup/suppl/doi:10.1073/pnas.1900544116/-/DCSupplemental.

Published online July 18, 2019.

Analysis of *Bdnf* transcript expression in 3-mo-old MKO mice revealed a ≤70% reduction in both oxidative and glycolytic skeletal muscle (Fig. 1*A* and *SI Appendix*, Fig. S1*A*). Interestingly, while *TrkB* levels were not affected by BDNF depletion, other NTs, such as *NT-3* and *NT-4/5*, show increased and decreased transcript expression, respectively, in the glycolytic gastrocnemius (GAS) muscle (*SI Appendix*, Fig. S1*A*). We, however, could not reveal changes in circulating BDNF; the latter was undetectable in mouse serum (*SI Appendix*, Fig. S1*B*) in agreement with previous studies (21, 22). Because BDNF is associated with fatty acid oxidation (17, 23, 24), we evaluated systemic and muscle metabolism of mice lacking muscle BDNF in a broad manner. MKO mice did not show an overt metabolic phenotype in terms of daily food intake (CTRL: 3.43 ± 0.11 g vs. MKO: 3.17 ± 0.26 g; $n = 5$ to 6; not significant), body, lean and fat mass, glucose tolerance, daily body temperature, VO_2 consumption, or energy substrate utilization (respiratory exchange ratio [RER]), which were all not significantly different from CTRL mice (*SI Appendix*, Fig. S1 *C–I*).

In line with unchanged whole-body lean mass, individual weights of different oxidative and glycolytic muscles were indistinguishable in BDNF MKO mice (*SI Appendix*, Fig. S1*E*). Basic histological evaluation of glycolytic tibialis anterior (TA) muscle revealed normal muscle structure (Fig. 1*B*). Using a telemetry system to record spontaneous, in-cage locomotion over a 10-d period, we observed that nighttime general locomotor activity was significantly reduced in MKO mice (Fig. 1*C*). A more detailed characterization of locomotor and gait behavior using the CatWalk XT system indicated that MKO gait velocity was slightly reduced as supported by parameters associated with walking speed (Fig. 1*D*). Overall, these data show that, even though spontaneous locomotion and walking speed are reduced in MKO mice, BDNF deletion is not linked to pathological changes in whole-body metabolism, body composition, and muscle mass and morphology.

Muscle-Specific BDNF Deletion Reduces Motor End Plate Volume in the Extensor Digitorum Longus Muscle. The BDNF-TrkB signaling pathway plays an essential role in the maturation and maintenance of the developing mammalian motor unit (6, 8, 13, 25). We thus investigated whether the locomotor phenotype of MKO mice was associated with NMJ abnormalities. We first evaluated the expression of transcripts playing a key role in the function and maintenance of the neuromuscular synapse and observed a significant reduction of the *Muscle-specific Kinase* (*MuSK*) and its downstream regulator *Docking Protein 7* (*Dok7*) in glycolytic muscles of MKO mice (Fig. 2*A* and *SI Appendix*, Fig. S2*A*). Of note, loss of MuSK abolishes synapse formation in mice (26). However, a closer examination of *MuSK* expression in subsynaptic regions—where it is preferentially expressed at the adult NMJ—did not reveal any significant reduction on BDNF deletion (*SI Appendix*, Fig. S2*A*). Moreover, MuSK protein showed a normal presence at synaptic sites, colocalizing with AChR clusters as in CTRL muscle (*SI Appendix*, Fig. S2*B*). Lastly, transcripts encoding for the α-and ε-AChR subunits were similarly enriched in the synaptic area of both genotypes (*SI Appendix*, Fig. S2*C*), further suggesting that molecules involved in NMJ maintenance are likely present at similar levels in adult MKO vs. CTRL muscles. Incidentally, transcript levels

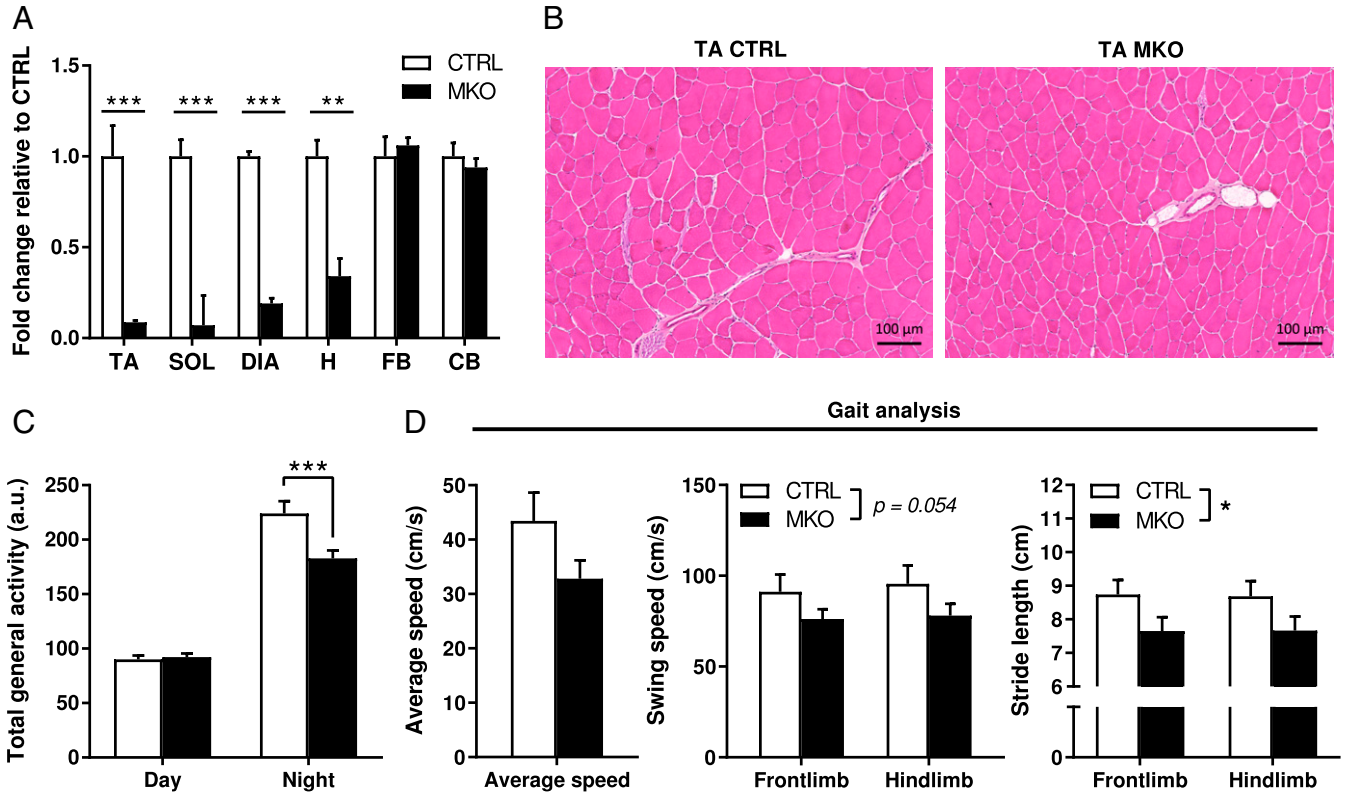

Fig. 1. BDNF MKO mice show altered spontaneous gait behavior and locomotion. (*A*) *Bdnf* gene expression in CTRL and BDNF MKO tissues. Expression values were determined by qPCR and normalized to *Hprt*. Data are shown as the average fold change ± SEM ($n = 3$ to 9 per genotype per tissue) relative to the expression in CTRL set to 1. CB, cerebellum; DIA, diaphragm; FB, forebrain; H, heart. (*B*) Histology of CTRL and MKO TA muscles as determined by hematoxylin and eosin staining. (Scale bar: 100 µm.) (*C*) Total gross locomotor activity ($n = 15$ per genotype, average of a 10-d period) and (*D*) gait locomotor parameters ($n = 8$ per genotype) of CTRL and MKO animals. Results are expressed as mean ± SEM. Unpaired Student's *t* test (*A* and *D*) and 2-way ANOVA followed by Sidak's multiple comparisons (*C* and *D*). $*P < 0.05$; $**P < 0.01$; $***P < 0.001$.

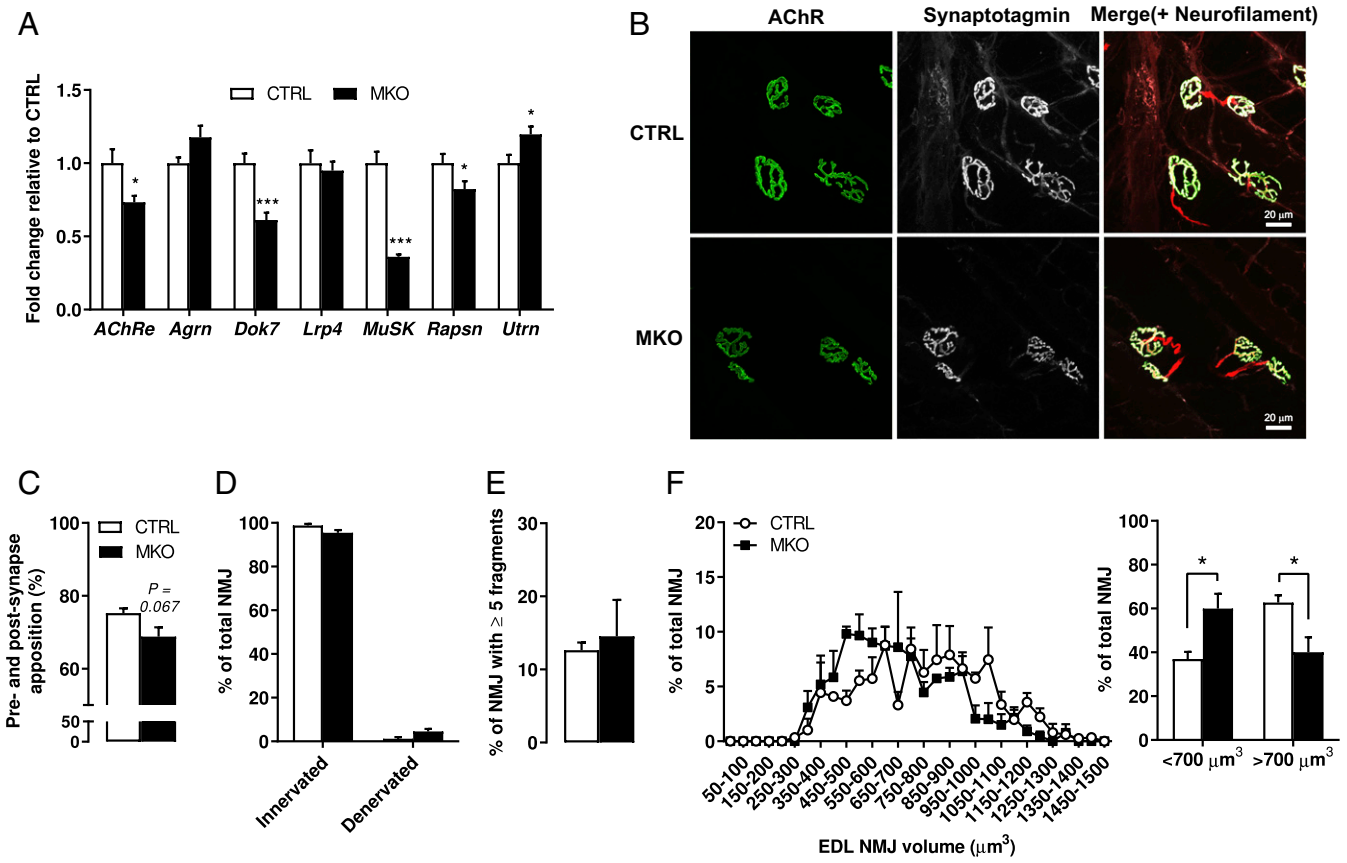

Fig. 2. Muscle-specific BDNF deletion reduces motor end plate size in the EDL muscle. (*A*) Gene expression in CTRL and BDNF MKO GAS muscles. Expression values were determined by qPCR and normalized to *Hprt*. Data are shown as the average fold change ± SEM ($n = 12$ per genotype) relative to the expression in CTRL set to 1. (*B*) Confocal microscopy images illustrating the apposition of both pre- and postsynaptic markers and the motor neuron innervation of EDL NMJs from CTRL and MKO mice. (Scale bar: 20 µm.) Quantification of (*C*) pre- and postsynapse apposition, (*D*) NMJ innervation, and (*E*) NMJ fragmentation. (*F*) NMJ volume distribution from CTRL and MKO EDL muscles (*Materials and Methods* has the number of NMJ analyzed per muscle per genotype). Results are expressed as percentage (mean ± SEM; $n = 4$ per genotype). Unpaired Student's *t* test (*A*, *C*, and *E*) and 2-way ANOVA followed by Sidak's multiple comparisons (*D* and *F*). $^{*}P < 0.05$; $^{***}P < 0.001$.

of *Bdnf* and *TrkB* were not enriched in microdissected synaptic regions of adult CTRL muscles (*SI Appendix*, Fig. S2*D*), hinting at synaptic and extrasynaptic functions of this signaling pathway.

We then examined the morphology of NMJs from the extensor digitorum longus (EDL)—a fast-twitch muscle used in rapid movements of hind limb digits—of CTRL and MKO animals by confocal microscopy. We used synaptotagmin, a synaptic vesicle-associated Ca^{2+} protein, as a presynaptic marker; α-bungarotoxin, a selective and potent ligand for AChR, to visualize the postsynaptic membrane; and an antineurofilament antibody to label motor nerve axons. Knockdown of muscle BDNF did not impair synapse structure in regard to presynaptic–postsynaptic apposition (Fig. 2 *B* and *C*). Similarly, no evidence of increased NMJ fragmentation and denervation was observed in MKO mice, indicating that muscle BDNF is not essential to maintain NMJ integrity (Fig. 2 *D* and *E*). Strikingly, however, lack of muscle BDNF led to a significant reduction of the motor end plate volume (Fig. 2*F*). Importantly, the reduction in NMJ volume was not associated with significant changes in the expression of $p75^{NTR}$ and both full-length and truncated forms of TrkB and TrkC in motor neurons and interneurons that lie in the lumbar portion of the spinal cord (*SI Appendix*, Fig. S2 *E–G*). Moreover, these receptors were not or only poorly detected in the GAS muscle (*SI Appendix*, Fig. S2 *E–G*), in keeping with their low expression levels postdifferentiation (16, 17, 27). In summary, muscle-specific ablation of BDNF does not affect NMJ apposition and integrity but evokes a shift in motor end plate size that is reminiscent of slow-type muscles (28).

Loss of BDNF Promotes Slow Contraction Velocity and Fatigue Resistance. We next assessed whether the morphological and molecular changes in the NMJs of MKO animals had any functional consequences on muscle contractile and fatigue properties and neuromuscular transmission. We first performed in situ measurements of TA muscle function in response to sciatic nerve stimulation. MKO muscles produced similar twitch and tetanic force as their CTRL counterparts (Fig. 3*A*, force frequency curve, and Fig. 3*E*, cross-sectional area [CSA]-normalized maximal twitch and tetanic forces), in line with in vivo measures of grip strength (*SI Appendix*, Fig. S2*J*). In contrast, time-to-peak tension and half-relaxation time were significantly longer in MKO mice (Fig. 3 *B–D*), indicating slower contraction velocities. Next, we studied force production during a fatigue protocol consisting of intermittent 100-Hz tetanic stimulations. After 1 min of repeated stimulation, contraction force started to drop faster in CTRL than in MKO TA muscles and remained lower until the end of the fatigue protocol (Fig. 3*F*). Consistent with fatigue resistance, BDNF knockout muscles recovered significantly faster than CTRL muscles, returning to ~95% of baseline peak force, while CTRL muscles reached ~84% of peak force 3 min after the fatigue protocol (Fig. 3*F*).

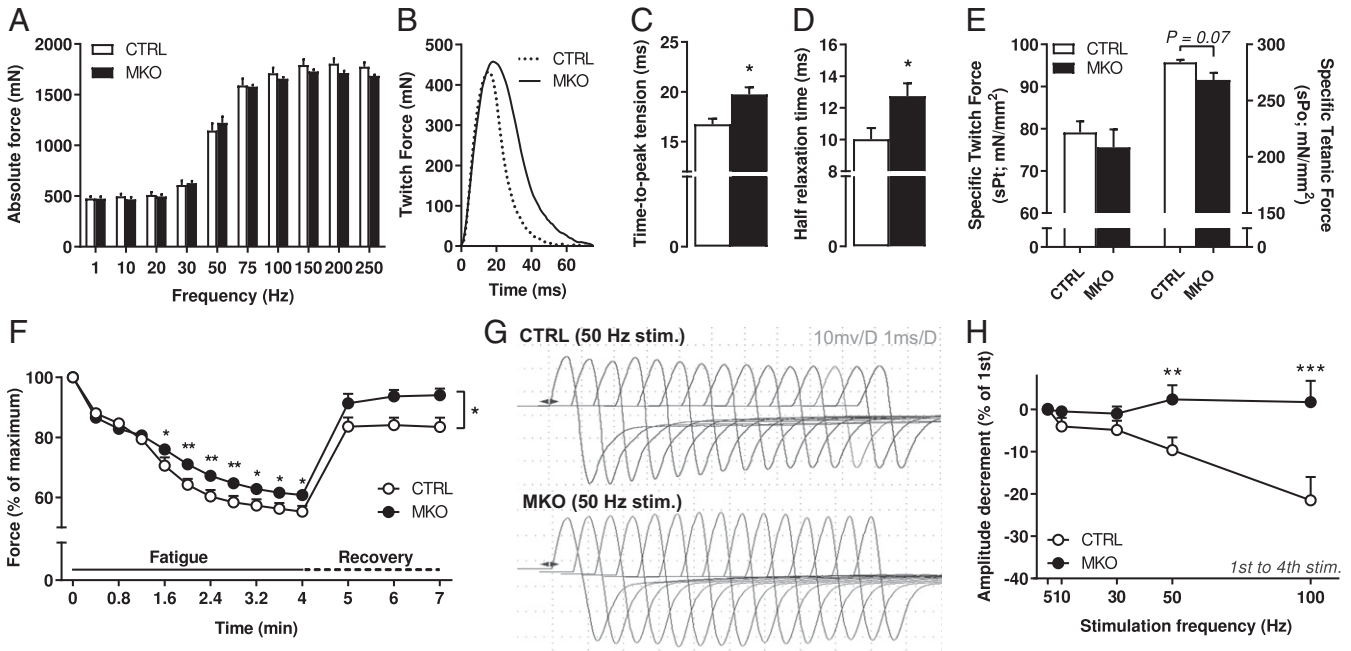

Fig. 3. Lack of BDNF promotes slow muscle contraction and enhances fatigue resistance. (*A*) In situ TA absolute muscle force frequency relationship as evoked by electrical sciatic nerve stimulation from CTRL ($n = 4$) and MKO ($n = 5$) mice. (*B*) Representative traces of twitch force from both genotypes. (*C*) Time-to-peak tension and (*D*) half-relaxation time. (*E*) CSA-normalized maximal twitch and tetanic forces. (*F*) Average curves showing the force decline during a 4-min muscle fatigue protocol and of muscle force recovery up to 3 min after fatigue. (*G*) Representative EMG traces from CTRL (*Upper*) and MKO (*Lower*) GAS muscle on 50-Hz stimulation of the sciatic nerve. (*H*) Average decrement in the amplitude of GAS CMAPs from 1st to 4th stimulation (5- to 50-Hz stimulation: $n = 9$ to 10 per genotype; 100-Hz stimulation: $n = 6$ per genotype). Results are expressed as percentage. Unpaired Student's *t* test (*C*–*E*) and 2-way ANOVA followed by Sidak's multiple comparisons (*A*, *F*, and *H*). $^{*}P < 0.05$; $^{**}P < 0.01$; $^{***}P < 0.001$.

To complement the in situ nerve–muscle stimulation experiments, we also evaluated in vivo evoked compound muscle action potentials (CMAPs) in the GAS muscle in response to supramaximal repetitive nerve stimulation using electromyography (EMG) as described previously (28). CMAPs did not significantly differ between genotypes over 15 consecutive stimuli at 5, 10, or 30 Hz (Fig. 3*H*). However, we found greater reductions of CMAPs at 50- and 100-Hz stimulation in CTRL than in MKO mice (Fig. 3 *G* and *H* and *SI Appendix*, Fig. S2*I*). Remarkably, while CMAPs dropped by ∼10 and ∼20% at 50- and 100-Hz stimulation, respectively, CMAPs reduction was completely absent after 4 stimulations in MKO mice (Fig. 3*H*). Lastly, to assess whether the changes in muscle contractile properties of MKO mice are associated with altered NMJ functionality, we evaluated both spontaneous and evoked neurotransmitter release using the levator auris longus (LAL)—a fast-twitch neck muscle—as described previously (29). Ex vivo electrophysiological recordings showed that the resting muscle membrane potential and both miniature end plate potential amplitude and frequency remained unaffected by muscle BDNF deletion (*SI Appendix*, Fig. S3 *A* and *B*, representative traces, and Tables S1 and S2). Likewise, there was no significant difference in the average amplitude of evoked neurotransmitter release, quantum content, and time constants between mouse groups (*SI Appendix*, Fig. S3 *C* and *D* and Table S3). Furthermore, short-term plasticity was indistinguishable between LAL NMJ synapses of CTRL vs. MKO animals (*SI Appendix*, Fig. S3 *E* and *F*). Together, these results indicate that glycolytic muscles lacking BDNF exhibit slower contractile properties and higher fatigue resistance in the absence of altered synaptic communication.

BDNF MKO Mice Show Improved Running Capacity. The change in NMJ morphology and the altered contractility in situ and using EMG collectively suggest a higher endurance performance. To test this, we first evaluated spontaneous wheel-running activity in both groups over a 7-d period. MKO mice exhibited a similar increase and overnight distribution of wheel activity as their CTRL littermates (*SI Appendix*, Fig. S4*A*). Because running performance as elicited by forced treadmill differs in many aspects from spontaneous mouse wheel-running activity, we then characterized the running capacity of MKO animals under dynamic treadmill exercise conditions. Untrained mice from both genotypes first performed a forced maximal running capacity test (i.e., VO_{2max} test) consisting of a speed increment of 2 m every 2 min at 15° inclination until exhaustion. In this strenuous exercise challenge, both genotypes demonstrated similar energy substrate utilization (RER) during the course of the experiment (*SI Appendix*, Fig. S4*B*). Furthermore, despite slightly higher VO_2 consumption rates toward the end of the running exercise session, muscle BDNF deletion did not significantly improve maximal aerobic capacity (*SI Appendix*, Fig. S4 *C* and *D*). Moreover, plasma lactate accumulation—a marker of muscle metabolism and fatigue—was similar in both genotypes at exhaustion (*SI Appendix*, Fig. S4*E*). Nevertheless, MKO mice were able to run significantly longer than CTRL mice (713 vs. 519 m; $n = 9$ per genotype; $P = 0.044$) (*SI Appendix*, Fig. S4 *G* and *H*). Incidentally, expression of exercise- and NT-related genes in response to an acute bout of treadmill exercise as described above was similar in the GAS muscle of both mouse genotypes (*SI Appendix*, Fig. S4 *I* and *J*).

Mice that performed the VO_{2max} test were then subjected to an endurance-type protocol, during which animals ran from 20 to 100% of their maximal running speed. Evaluation of energy fuel utilization and oxygen consumption, specifically at moderate exercise intensities [i.e., 20 to 60% of maximal speed when muscle fat oxidation is at its highest (30, 31)] did not reveal any differences between genotypes (Fig. 4 *A* and *B*). Moreover, blood lactate levels were similarly increased in both genotypes at

exhaustion (Fig. 4*C*). Conversely, blood glucose values were significantly lower in MKO mice at exhaustion (Fig. 4*D*), which could result from their altered performance. Indeed, in line with their improved maximal running capacity, BDNF MKO animals demonstrated significantly greater endurance performance, running about 1.5 times the distance of CTRL mice (BDNF MKO: 2,708 m; CTRL: 1,862 m; $P = 0.015$) (Fig. 4 *F* and *G*). In summary, deletion of BDNF in mouse skeletal muscle confers greater resistance to fatigue during physical exercise without significantly affecting whole-body aerobic capacity and energy substrate utilization.

Lack of Muscle BDNF Promotes a Fast-to-Slow Transition in Glycolytic Muscles. Muscle fiber type and oxidative capacity are essential determinants of muscle contractile properties, endurance, and fatigue (32). Therefore, we assessed whether BDNF deletion was associated with a muscle fiber transformation. Fiber composition and CSA were unchanged in the oxidative soleus (SOL) muscle of MKO mice (*SI Appendix*, Fig. S5 *A–C*). In contrast, the proportion of type IIX fibers in both glycolytic TA and EDL muscles was significantly increased in MKO animals at the expense of type IIB fibers (Fig. 5 *A* and *B*). Importantly, type IIX fibers show characteristics intermediate to types IIA and IIB fibers (e.g., in terms of contraction velocities and resistance to fatigue as evaluated above) and succinate dehydrogenase activity—a mitochondrial enzyme involved in oxidative phosphorylation (33). Accordingly, we observed that muscles depleted of BDNF showed higher succinate dehydrogenase (SDH) activity-dependent staining (Fig. 5*C*). Of note, the higher proportion of type IIX fibers in both TA and EDL muscles of MKO mice was not associated with significant change in myofiber CSA (Fig. 5*D*).

To investigate whether other fiber type-specific genes were also affected by this transition from type IIB to IIX, we measured the expression of several key oxidative and glycolytic markers by qPCR. In line, the α-cardiac form of the actin gene (*Actc1*)—a major constituent of the contractile apparatus predominantly expressed in oxidative muscles (34)—was elevated in the absence of BDNF (Fig. 5*E*). Conversely, the glycolytic marker *troponin-C fast* (*Tnnc2*) and transcriptional regulators controlling glycolytic fiber identity, such as *Baf60c*/*Smarcd3* (35) and *Tbx15* (36), were down-regulated in MKOs (Fig. 5*E*). The higher proportion of type IIX fibers was, however, not associated with elevated expression of *Ppargc1b* (37) or increased mitochondrial transcript and mitochondrial DNA levels (*SI Appendix*, Fig. S5*D*). We also examined the level of transcripts encoding key sarcoplasmic calcium-regulatory proteins in muscles of MKO mice. In particular, the fast-type calcium-transporting ATPase *Atp2a1* (also called sarco/endoplasmic reticulum Ca^{2+}-ATPase 1 [*Serca1*]) was reduced, while the slow-type form *Atp2a2* (*Serca2*) was significantly increased (Fig. 5*F*). In contrast, both the fast-type calsequestrin 1 (*Casq1*) and the slow-type *Casq2* were elevated in the MKO animals (Fig. 5*F*). Additional transcripts encoding for regulators of fast fiber Ca^{2+} homeostasis (e.g., myoregulin [*Mrln*]—a repressor of SERCA activity expressed in fast fibers [38]—and ryanodine receptor [*RyR1*] and parvalbumin [*Pvalb*]—highly expressed in fast-contracting fibers that have a more developed sarcoplasmic reticulum [33]) equally showed significantly reduced expression levels in muscle cells depleted of BDNF (Fig. 5*F*). These results collectively demonstrate that muscle-derived BDNF depletion promotes a fast-to-slow transition in glycolytic muscles.

BDNF Overexpression Increases Fast-Type Gene Expression and Glycolytic Fibers. The effect of muscle BDNF deletion on fiber-type composition prompted us to investigate the consequence of enhanced BDNF expression in skeletal muscle of adult CTRL mice. To this aim, a plasmid-based gene delivery method was used to introduce either BDNF or an empty vector (EV) into the TA muscle by electroporation. *SI Appendix*, Fig. S6*A* depicts in vivo transfection efficiency of a pCAG-EGFP (enhanced green fluorescent protein) expression vector using our established parameters, demonstrating even muscle distribution of EGFP at 7 and 21 d postelectroporation. Importantly, when TA muscles

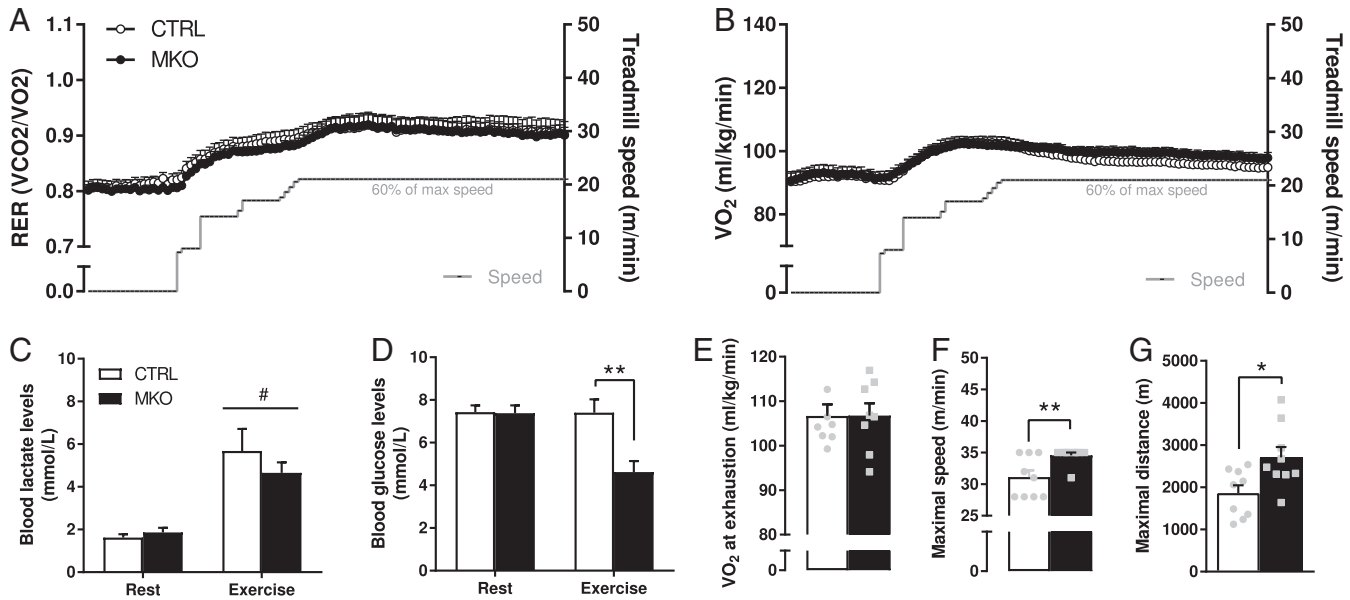

Fig. 4. BDNF MKO mice show improved running endurance capacity. (*A*) RER and (*B*) O_2 consumption as a function of speed in CTRL and MKO animals during endurance exercise challenge. Note that data in *A* and *B* are only depicted until a speed of 22 m/min (i.e., 60% of maximum speed). (*C*) Blood lactate and (*D*) glucose levels at rest and within 1 min after exhaustion. (*E*) Maximal O_2 consumption at exhaustion. (*F*) Maximal speed and (*G*) total distance reached at exhaustion. Results are expressed as mean ± SEM ($n = 9$ per genotype except in *A*, *B*, and *E*, where data from 1 CTRL and 1 MKO mouse could not be included due to O_2 artifacts during run acquisition). Unpaired Student's *t* test (*E–G*) and 2-way ANOVA followed by Sidak's multiple comparisons (*C* and *D*). $^*P < 0.05$; $^{**}P < 0.01$; $^{\#}$Significant difference ($P < 0.05$) between experimental conditions.

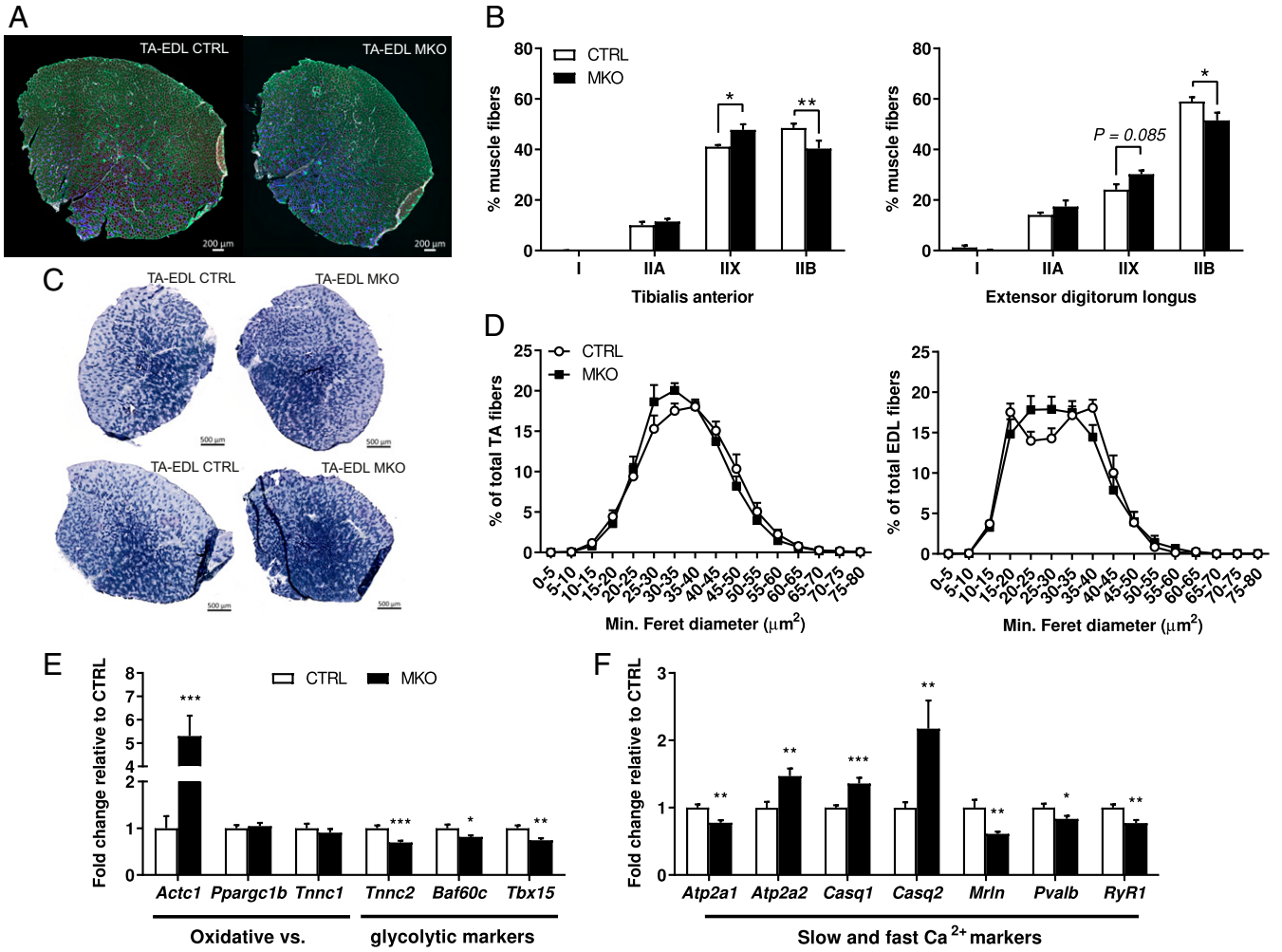

Fig. 5. Lack of BDNF leads to a type IIB to IIX transition in glycolytic muscles. (*A*) Representative fluorescence microscopy images illustrating the fiber-type composition in the TA-EDL muscle of CTRL and MKO animals. Corresponding color legend for fiber types: type I = red, type IIA = blue, type IIX = unstained (black), type IIB = green, and laminin = white. (Scale bar: 200 μm.) (*B*) Quantification of fiber-type content in (*Left*) TA and (*Right*) EDL muscles ($n = 5$ per genotype). Note that EDL and TA muscles were analyzed separately. (*C*) Representative SDH staining of TA-EDL muscles from different CTRL and MKO animals. (Scale bar: 500 μm.) (*D*) CSA based on minimal Feret's diameter of (*Left*) TA and (*Right*) EDL myofibers ($n = 5$ per genotype). Results are expressed as percentage (mean ± SEM). (*E* and *F*) Gene expression in CTRL and BDNF MKO GAS muscles. Expression values were determined by qPCR and normalized to *Hprt*. Data are shown as the average fold change ± SEM ($n = 12$ per genotype) relative to the expression in CTRL set to 1. Unpaired Student's *t* test (*E* and *F*) and 2-way ANOVA followed by Sidak's multiple comparisons (*B* and *D*). $^*P < 0.05$; $^{**}P < 0.01$; $^{***}P < 0.001$.

from CTRL mice were transfected with a BDNF-encoding vector, both pro- and mature forms of BDNF were detected 21 d after electrotransfer with 2 different antibodies (Fig. 6*A*). This clearly indicates that—alongside the drastic elevation of its transcript (Fig. 6*B*)—BDNF is further processed and cleaved in adult skeletal muscle.

Next, we found that BDNF elevation mirrored the consequences of BDNF deletion at the gene expression level. Specifically, there was a greater expression of glycolytic markers (e.g., *Serca1* and its coregulator *Mlrn*) and of transcriptional mediators of fast fiber-type gene programs, such as *Baf60c* and *Tbx15* (Fig. 6 *B* and *C*). Because electroporation is known to produce significant damage in skeletal muscle leading to satellite cell activation and the formation of new fibers (39–41), we concomitantly determined myosin heavy-chain composition in both small new fibers (i.e., based on a CSA value < 20 μm²), nearly absent in nonelectroporated TA muscle (Fig. 5*D*), and in larger fibers (CSA > 20 μm²) of EV- and BDNF-electroporated muscles (Fig. 6*D*). Intriguingly, on BDNF overexpression, small myofibers had a significantly lower content of the type IIX myosin heavy-chain isoform alongside an elevation of the type IIB isoform (Fig. 6*E*). Thus, overexpression of BDNF is sufficient to induce fast-twitch markers and influence fiber-type composition in skeletal muscle.

Higher Muscle Mass, Strength, and Oxidative Fibers in Old BDNF MKO Mice. NMJ structure, muscle fiber type and contractile properties, fatigue resistance, and exercise capacity are all changed in young adult BDNF MKO animals. Incidentally, altered NT signaling at the neuromuscular interface is associated with the age-related decline of muscle mass and function (15, 16, 42). Moreover, there is an age-dependent decrease of both circulating BDNF and brain *TrkB* levels in humans (43, 44) and a likewise age-dependent reduction of both *Bdnf* and *TrkB* levels in the rodent brain (45–47). However, we could not find data on muscle *Bdnf* and *TrkB* expression in the aging context and have, therefore, compared their transcript levels in 6- vs. 24-mo-old CTRL animals. We did not find any change in regard to *Bdnf* and *TrkB* expression in the old muscle (Fig. 7*A*).

In a last set of experiments, we evaluated whether the lifelong deletion of muscle BDNF would further alter muscle physiology

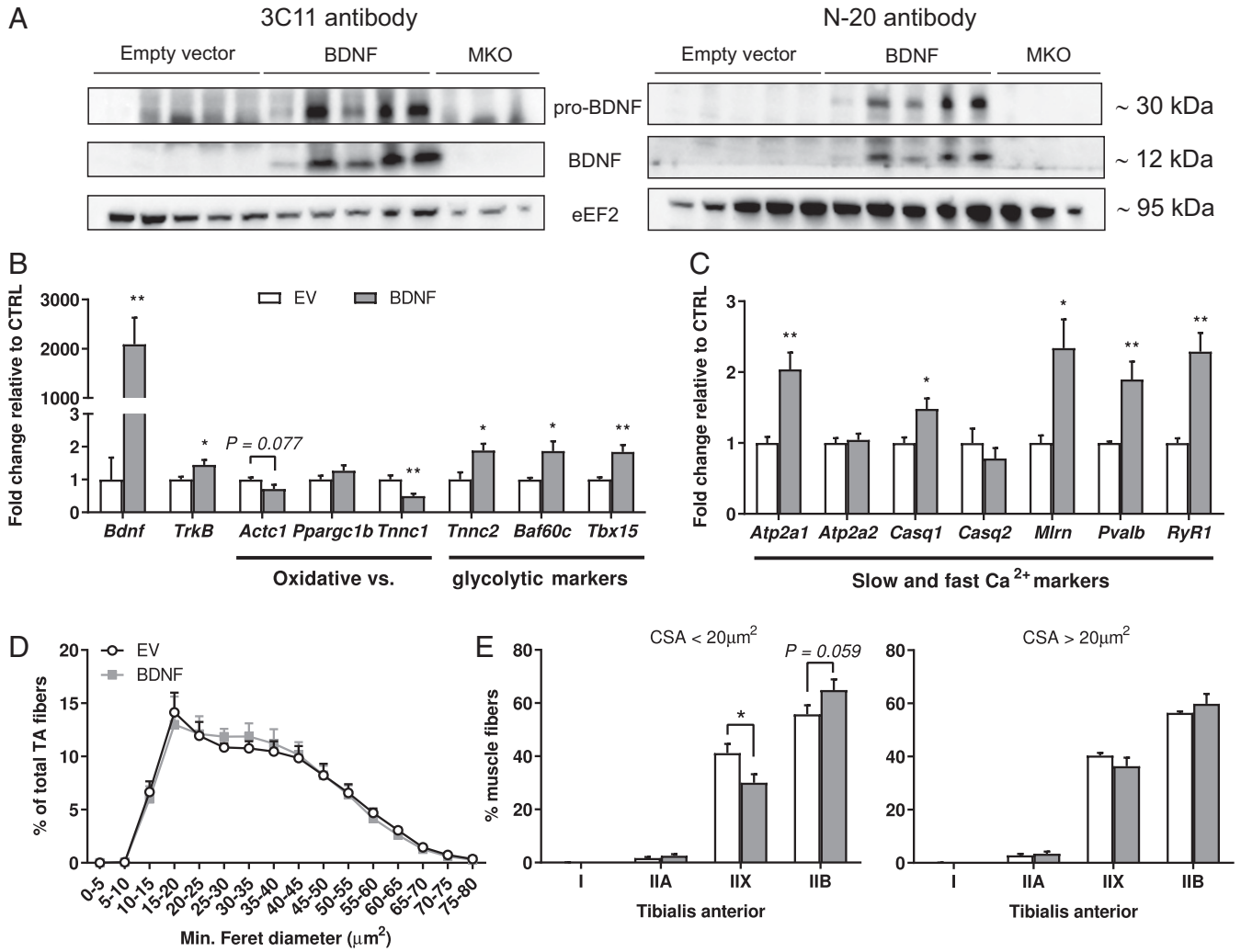

Fig. 6. BDNF influences skeletal muscle fiber-type specification. (*A*) Expression of BDNF protein in EV- and BDNF-electroporated TA muscles ($n = 5$ per condition) as determined by western blot. Note that muscle protein extracts from MKO animals were used as negative controls. (*B* and *C*) Gene expression in EV- and BDNF-electroporated TA muscles. Expression values were determined by qPCR and normalized to *Hprt*. Data are shown as the average fold change ± SEM ($n = 5$ per condition) relative to the expression in EV set to 1. (*D*) CSA based on minimal Feret's diameter of TA myofibers ($n = 5$ per genotype). (*E*) Fiber-type composition in small (*Left*) vs. large (*Right*) TA fibers ($n = 5$ per genotype). Results are expressed as percentage (mean ± SEM). Unpaired Student's *t* test (*B* and *C*) and 2-way ANOVA followed by Sidak's multiple comparisons (*E*). $*P < 0.05$; $**P < 0.01$.

in the aging context. Motor balance and coordination were unchanged in 24-mo-old MKO mice (Fig. 7 *B* and *C*). Likewise, old MKO animals demonstrated a running capacity comparable with their CTRL littermates (Fig. 7*D*). Old MKO mice, however, showed significantly higher grip strength in comparison with old CTRL mice (Fig. 7*E*). This was, furthermore, associated with significantly increased whole-body lean mass alongside elevated GAS and quadriceps hind limb muscle mass (Fig. 7 *F* and *G*). Finally, we found a higher SDH activity-dependent staining and a significantly increased proportion of type IIA fibers in TA muscles of 24-mo-old MKO mice (Fig. 7 *H* and *I*). Overall, these results suggest that lifelong expression of muscle BDNF is not required for the maintenance of neuromuscular function and that, conversely, the more oxidative phenotype of muscles lacking BDNF contributes to attenuation of some aspects of muscle aging.

Discussion

The trophic activity of BDNF and related NT family members is well recognized in the interaction between cells of the central nervous system (24, 48). In contrast, the regulation and function of BNDF in other cell types remains less understood. Here, we describe a hitherto unknown and surprising effect of skeletal muscle BNDF on the promotion of a fast-twitch glycolytic muscle fiber program using both loss- and gain-of-function approaches in vivo.

Our findings uncover BDNF as a myokine that promotes a glycolytic fiber phenotype; other factors, such as the insulin-like growth factor 2 (IGF2), have been associated with embryonic development of fast fibers (49), while IGF1 primarily promotes hypertrophy of fibers, with minimal effects on fiber-type distribution (50). In contrast, our data demonstrate that BDNF affects the gene program and fiber composition of glycolytic muscles without significantly altering muscle fiber CSA. It is, therefore, conceivable that BNDF cooperates with other factors (e.g., IGF1) in the adaptation of skeletal muscle to resistance training. Of note, the seemingly beneficial effect of muscle-specific deletion of BDNF on different parameters (e.g., fatigue resistance and endurance capacity) might be offset in other contexts. It thus will be interesting to test the performance of the BDNF MKO animals in other paradigms where adequate function of type IIB fibers is required (e.g., maximal strength or resistance

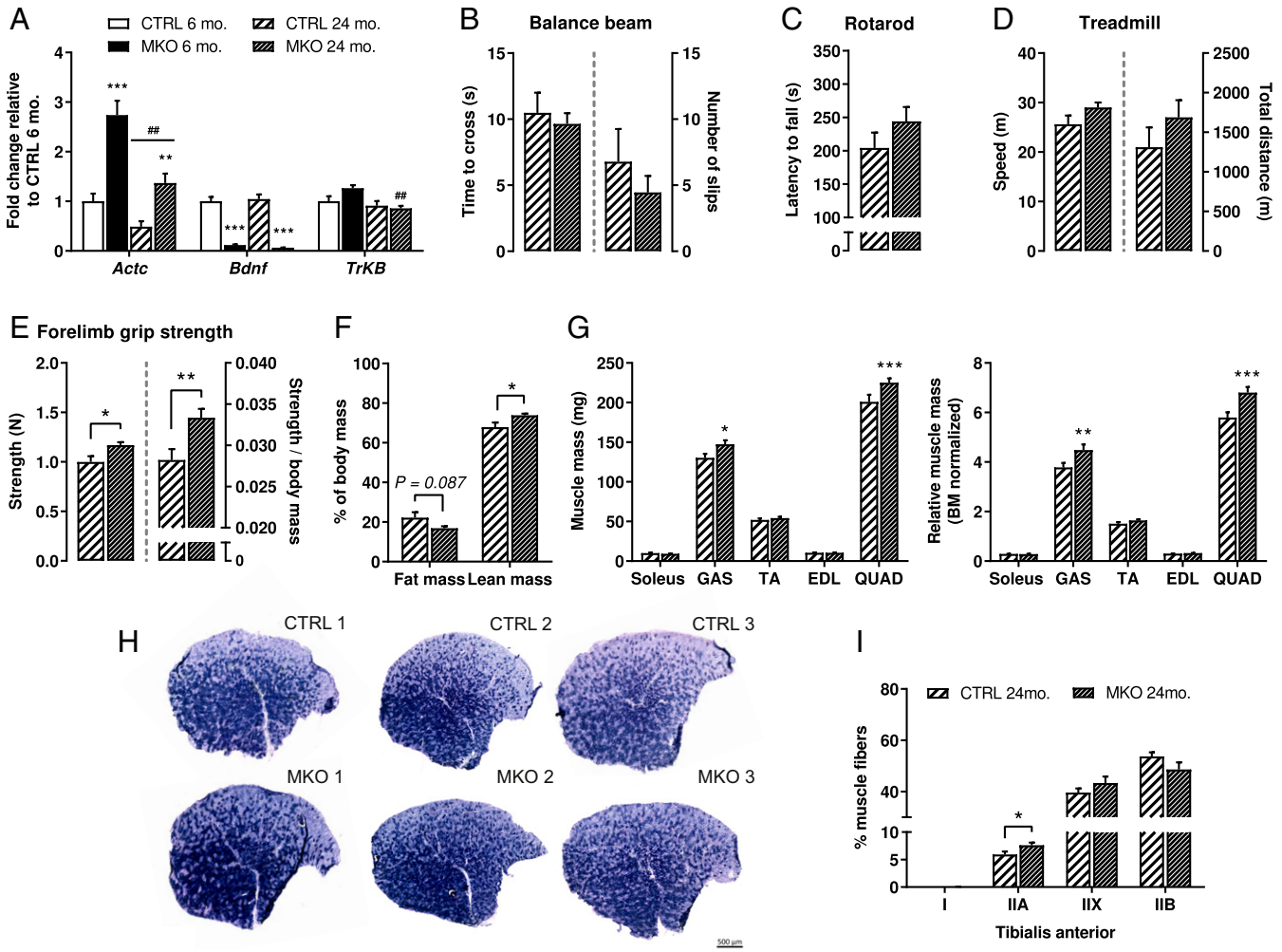

Fig. 7. The 24-mo-old BDNF MKO mice show higher muscle mass, grip strength, and oxidative fiber number. (*A*) Gene expression in young ($n = 6$ per genotype) and old ($n = 7$ to 9 per genotype) CTRL and BDNF MKO GAS muscles. Expression values were determined by qPCR and normalized to *Hprt*. Data are shown as the average foldchange ± SEM relative to the expression in young CTRL set to 1. (*B*) Balance beam (CTRL $n = 9$, MKO $n = 11$), (*C*) rotarod (CTRL $n = 9$, MKO $n = 12$), and (*D*) treadmill running data (CTRL $n = 8$, MKO $n = 9$). (*E*) Absolute and body mass-normalized forelimb muscle strength as determined by grip test (CTRL $n = 9$, MKO $n = 12$). Note that experiments were performed from the age of 23 mo and that some mice from this specific cohort spontaneously died between the start of our behavioral investigation and their euthanasia. (*F*) Normalized lean and fat mass and (*G*) absolute vs. normalized muscle mass from 24-mo-old CTRL ($n = 7$) and MKO ($n = 9$) animals just before euthanasia. QUAD, quadricep. (*H*) Representative SDH staining of TA muscles from different old CTRL and MKO animals. Note that sections with the same number originate from the same slide. (Scale bar: 500 μm.). (*I*) Evaluation of TA muscle fiber composition of old CTRL and MKO animals ($n = 6$ per genotype from randomly chosen muscles). Results are expressed as mean ± SEM. Unpaired Student's *t* test (*B*–*E*) and 2-way ANOVA followed by Sidak's multiple comparisons (*A*, *F*, *G*, and *I*). $^{*}P < 0.05$; $^{**}P < 0.01$; $^{***}P < 0.001$; $^{\#\#}$Significant difference ($P < 0.01$) between conditions.

exercise performance). Nevertheless, other pathological settings could profit from a reduction or ablation of muscle BNDF as evidenced by the improvement of lean mass, muscle weight, and grip strength in old mice.

Contrary to postnatal and whole-body disruption of TrkB (6, 15, 25), muscle-specific BDNF deletion did not adversely affect neuromuscular structure and function. Furthermore, even though we did not directly assess NMJ morphology and functionality in old MKO animals, the fact that these mice displayed similar, if not greater, muscle force, motor balance, and coordination likely rules out an essential role for postsynaptic BDNF expression in the lifelong maintenance of the motor unit. Finally, our observations of unchanged substrate utilization on BDNF deletion are contrasting with the proposed role of BDNF as an exercise-induced myokine to regulate fatty acid oxidation (17). Whether this difference stems from diverging effects of long-term deletion (these results) vs. the transient overexpression and the relatively modest induction of BDNF after acute exercise bouts (17) remains unclear. In any case, in contrast to its key function in other central and peripheral cells controlling energy homeostasis (23, 24), BDNF depletion did not alter systemic energy homeostasis. One limitation of this study, however, is the use of the HSA-Cre transgene to excise BDNF, leading to Cre expression from E9.5 in somitic cells committed to the myogenic lineage (19, 20). It thus would be interesting to initiate muscle BDNF deletion at a later stage to rule out the possibility of any developmental compensation (51).

Some of the characteristics of muscle lacking BDNF (e.g., higher SDH activity, slower contraction and relaxation times, and decreased fatigability rate) are found in endurance-trained muscle (52). However, MKO mice did not show increased spontaneous locomotor activity but rather, showed decreased spontaneous locomotor activity—as some other mouse models

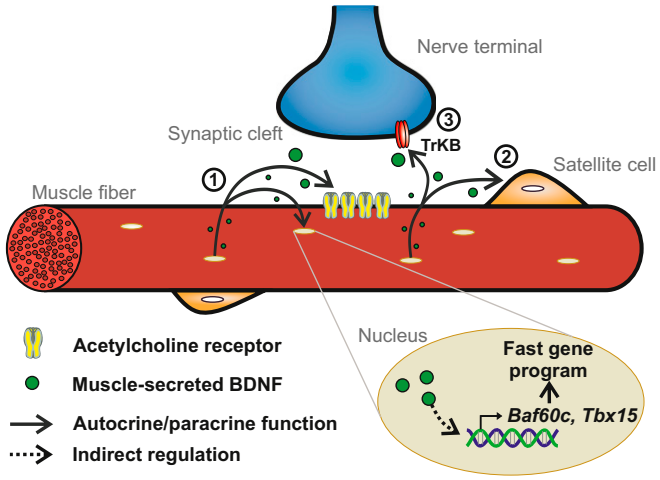

Fig. 8. Proposed model by which BDNF signaling regulates neuromuscular physiology. (*1*) BDNF could act as an autocrine factor to influence the expression of transcriptional regulators involved in fast-twitch muscle-specific gene expression or the expression of synaptic proteins involved in AChR clustering. (*2*) As a paracrine factor, BDNF could regulate the differentiation of satellite cells into slow vs. fast myofibers. (*3*) BDNF might also affect myofiber identity and motor end plate structure indirectly (e.g., by modulating the activity of the TrkB receptors present in nerve terminals of motor neurons).

exhibiting a slow-type muscle transition (36, 53)—ruling out physical activity as a primary cause of the fiber-type change. Intriguingly, there is a clear relationship between the expression of the fast IIB myosin isoform and BDNF during early postnatal development, when muscles are subjected to distinct programs of myosin isoform transitions influenced, for example, by functional demand or motor innervation (33, 54). For instance, the fast IIB myosin isoform rises in both mouse EDL and GAS muscles from day 5 until day 90 after birth (54). BDNF protein also gradually increases in glycolytic muscles of rodent neonates but not in the SOL (27, 55). Besides, combined administration of a ciliary neurotrophic factor (CNTF)–BDNF mixture after neonatal sciatic nerve crush injury can rescue a small fraction (i.e., 5%) of type IIB fibers in the EDL muscle (27). Mechanistically, it is not clear how BNDF controls the type IIB fiber program. Future studies will aim at elucidating the BDNF-activated signaling pathways that ultimately result in a transcriptional induction of *Baf60c* and *Tbx15*, 2 transcriptional regulators involved in fast-twitch muscle-specific gene expression (35, 36). BDNF might also affect these regulators indirectly [e.g., by modulating the activity of the TrkB receptors present in nerve terminals of motor neurons (5, 6)] to mediate morphological remodeling of the NMJ. In that regard, other approaches to overexpress BDNF [e.g., the tetracycline-inducible system (56)] could not only circumvent the significant changes induced by muscle electroporation but also, allow the careful functional and structural evaluation of the effect of muscle BDNF elevation at different developmental stages on the neuromuscular system. Finally, the role of extrinsic signals, such as muscle-derived BDNF, in influencing the commitment of myoblast nuclei to particular gene expression programs and thus, the differentiation of these cells into slow vs. fast myofibers needs additional investigation (Fig. 8).

In summary, we report here that BDNF is a myokine that regulates glycolytic muscle fiber-type identity. Muscle-specific loss of BDNF confers beneficial effects on endurance and mitigates loss of muscle mass and function in sarcopenia. Thus, strategies aimed at neutralizing muscle BDNF might be of interest in certain pathologies. Inversely, our findings of BNDF to promote type IIB fiber programs could be leveraged in diseases where the function of glycolytic muscle fibers is compromised or increased fast-twitch muscle fiber activity is desirable. For example, circulating BDNF levels are associated with type 2 diabetes (16, 57, 58), and chronic BDNF administration enhances glucose uptake in muscle cells (59), which could be, at least in part, mediated by a higher proportion of glycolytic type IIB muscle fibers. Moreover, BDNF may also modulate the glycolytic capabilities of muscle fibers by mechanisms similar to the fibroblast growth factor 21 myokine (60, 61). Lastly, in light of the susceptibility of certain muscle fibers to muscle diseases [e.g., Duchenne muscular dystrophy (62)] and the positive effect of essential determinants of fiber identity on muscle disease progression (63, 64), our findings warrant additional studies to determine whether modulating the activity of BDNF represents an effective therapeutic strategy to delay or even prevent muscle wasting disorders.

Materials and Methods

Animals. *HSA-Cre* transgenic mice were purchased from the Jackson Laboratory (stock no. 006149). *Bdnf*$^{flox/flox}$ mice were a gift from Yves-Alain Barde, Cardiff University, Wales, United Kingdom and have been previously characterized (ref. 65 has mutation and genotyping details). Mice were maintained on a C57BL/6J genetic background in the animal facility of the Biozentrum (University of Basel) in a temperature-controlled room (21 °C to 22 °C) under a 12:12-h light/dark cycle (lights on at 6:00 AM). Unless specifically mentioned, all experiments were performed in young adult male mice (3 to 4 mo old) housed in groups of 3 to 5 in standard cages with enrichment and free access to regular chow diet (3432; KLIBA NAFAG) and water. All experiments were performed in accordance with the principles of the Basel Declaration and with Federal and Cantonal Laws regulating the care and use of experimental animals in Switzerland as well as institutional guidelines of the Biozentrum and the University of Basel. The protocol with all methods described here was approved by the Kantonales Veterinäramt of the Kanton Basel-Stadt under consideration of the wellbeing of the animals and the 3R (replacement, reduction, and refinement) principle.

Statistical Analysis. No statistical methods were used to predetermine sample size. The *n* number used per genotype for each experiment is indicated in the figure legends. Data are expressed as mean ± SEM and were represented and analyzed with the GraphPad Prism 7.0 software. Comparisons between 2 groups were performed with unpaired Student's *t* test. For assessment between 2 independent variables, 2-way ANOVA was used followed by Sidak's multiple comparisons test if the interaction term was significant. A value of $P < 0.05$ was considered statistically significant. Symbols used to indicate the different degrees of statistical significance are as follow: $^{*}P < 0.05$, $^{**}P < 0.01$, and $^{***}P < 0.001$ between mouse genotypes and $^{\#}P < 0.05$ and $^{\#\#}P < 0.01$ between experimental conditions.

Details about body composition analysis; comprehensive laboratory animal monitoring system, glucose homeostasis, body temperature and locomotor activity recordings, gait analysis, indirect calorimetry coupled to treadmill exercise, repetitive nerve stimulation EMG, muscle force and fatigue measurements, muscle electroporation, tissue collection, enzyme-linked immunosorbent assay, histology and immunohistochemistry, slide imaging and image analysis, muscle RNA extraction and real-time qPCR, protein extraction and western blot, mitochondrial DNA number, laser capture microdissection, electrophysiology, behavioral phenotyping of old mice, and antibodies and reagents are provided in *SI Appendix, Supplementary Materials and Methods*. Primer pairs and TaqMan probes used in this study are listed in *SI Appendix*, Table S4.

ACKNOWLEDGMENTS. We thank the Imaging Core Facility of the Biozentrum for their technical help with imaging procedures and data analysis. We also thank Prof. Yves-Alain Barde (Cardiff University, Wales, United Kingdom) for providing the founder *Bdnf*$^{flox/flox}$ mice. L.T. is supported by Spanish Ministry of Economy and Competitiveness/European Regional Development Fund BFU2016-78934-P. The work in the laboratory of C.H. is funded by the Swiss National Science Foundation, European Research Council Consolidator Grant 616830-MUSCLE_NET, Swiss Cancer Research Grant KFS-3733-08-2015, the Swiss Society for Research on Muscle Diseases, SystemsX.ch, the Novartis Stiftung für Medizinisch-Biologische Forschung, and the University of Basel.

1. M. V. Chao, Neurotrophins and their receptors: A convergence point for many signalling pathways. *Nat. Rev. Neurosci.* **4**, 299–309 (2003).
2. E. J. Huang, L. F. Reichardt, Trk receptors: Roles in neuronal signal transduction. *Annu. Rev. Biochem.* **72**, 609–642 (2003).
3. G. Chevrel, R. Hohlfeld, M. Sendtner, The role of neurotrophins in muscle under physiological and pathological conditions. *Muscle Nerve* **33**, 462–476 (2006).
4. B. Kablar, M. A. Rudnicki, Development in the absence of skeletal muscle results in the sequential ablation of motor neurons from the spinal cord to the brain. *Dev. Biol.* **208**, 93–109 (1999).
5. N. Garcia *et al*., The interaction between tropomyosin-related kinase B receptors and presynaptic muscarinic receptors modulates transmitter release in adult rodent motor nerve terminals. *J. Neurosci.* **30**, 16514–16522 (2010).
6. M. Gonzalez *et al*., Disruption of Trkb-mediated signaling induces disassembly of postsynaptic receptor clusters at neuromuscular junctions. *Neuron* **24**, 567–583 (1999).
7. L. B. Tovar-Y-Romo, U. N. Ramírez-Jarquín, R. Lazo-Gómez, R. Tapia, Trophic factors as modulators of motor neuron physiology and survival: Implications for ALS therapy. *Front. Cell. Neurosci.* **8**, 61 (2014).
8. V. E. Koliatsos, R. E. Clatterbuck, J. W. Winslow, M. H. Cayouette, D. L. Price, Evidence that brain-derived neurotrophic factor is a trophic factor for motor neurons in vivo. *Neuron* **10**, 359–367 (1993).
9. S. Capsoni, F. Ruberti, E. Di Daniel, A. Cattaneo, Muscular dystrophy in adult and aged anti-NGF transgenic mice resembles an inclusion body myopathy. *J. Neurosci. Res.* **59**, 553–560 (2000).
10. P. Ernfors, K. F. Lee, J. Kucera, R. Jaenisch, Lack of neurotrophin-3 leads to deficiencies in the peripheral nervous system and loss of limb proprioceptive afferents. *Cell* **77**, 503–512 (1994).
11. R. Klein *et al*., Disruption of the neurotrophin-3 receptor gene trkC eliminates la muscle afferents and results in abnormal movements. *Nature* **368**, 249–251 (1994).
12. N. Belluardo *et al*., Neuromuscular junction disassembly and muscle fatigue in mice lacking neurotrophin-4. *Mol. Cell. Neurosci.* **18**, 56–67 (2001).
13. D. G. Wells, B. A. McKechnie, S. Kelkar, J. R. Fallon, Neurotrophins regulate agrin-induced postsynaptic differentiation. *Proc. Natl. Acad. Sci. U.S.A.* **96**, 1112–1117 (1999).
14. H. S. Je *et al*., ProBDNF and mature BDNF as punishment and reward signals for synapse elimination at mouse neuromuscular junctions. *J. Neurosci.* **33**, 9957–9962 (2013).
15. S. A. Kulakowski, S. D. Parker, K. E. Personius, Reduced TrkB expression results in precocious age-like changes in neuromuscular structure, neurotransmission, and muscle function. *J. Appl. Physiol.* **111**, 844–852 (2011).
16. K. Sakuma, A. Yamaguchi, The recent understanding of the neurotrophin's role in skeletal muscle adaptation. *J. Biomed. Biotechnol.* **2011**, 201696 (2011).
17. V. B. Matthews *et al*., Brain-derived neurotrophic factor is produced by skeletal muscle cells in response to contraction and enhances fat oxidation via activation of AMP-activated protein kinase. *Diabetologia* **52**, 1409–1418 (2009).
18. C. Clow, B. J. Jasmin, Brain-derived neurotrophic factor regulates satellite cell differentiation and skeltal muscle regeneration. *Mol. Biol. Cell* **21**, 2182–2190 (2010).
19. M. Leu *et al*., Erbb2 regulates neuromuscular synapse formation and is essential for muscle spindle development. *Development* **130**, 2291–2301 (2003).
20. M. Schwander *et al*., β1 integrins regulate myoblast fusion and sarcomere assembly. *Dev. Cell* **4**, 673–685 (2003).
21. P. Chacón-Fernández *et al*., Brain-derived neurotrophic factor in megakaryocytes. *J. Biol. Chem.* **291**, 9872–9881 (2016).
22. A. B. Klein *et al*., Blood BDNF concentrations reflect brain-tissue BDNF levels across species. *Int. J. Neuropsychopharmacol.* **14**, 347–353 (2011).
23. S. Bathina, U. N. Das, Brain-derived neurotrophic factor and its clinical implications. *Arch. Med. Sci.* **11**, 1164–1178 (2015).
24. E. E. Noble, C. J. Billington, C. M. Kotz, C. Wang, The lighter side of BDNF. *Am. J. Physiol. Regul. Integr. Comp. Physiol.* **300**, R1053–R1069 (2011).
25. C. B. Mantilla *et al*., TrkB kinase activity maintains synaptic function and structural integrity at adult neuromuscular junctions. *J. Appl. Physiol.* **117**, 910–920 (2014).
26. T. M. DeChiara *et al*., The receptor tyrosine kinase MuSK is required for neuromuscular junction formation in vivo. *Cell* **85**, 501–512 (1996).
27. K. Mousavi, B. J. Jasmin, BDNF is expressed in skeletal muscle satellite cells and inhibits myogenic differentiation. *J. Neurosci.* **26**, 5739–5749 (2006).
28. A.-S. Arnold *et al*., Morphological and functional remodelling of the neuromuscular junction by skeletal muscle PGC-1α. *Nat. Commun.* **5**, 3569 (2014).
29. R. Tejero, M. Lopez-Manzaneda, S. Arumugam, L. Tabares, Synaptotagmin-2, and -1, linked to neurotransmission impairment and vulnerability in Spinal Muscular Atrophy. *Hum. Mol. Genet.* **25**, 4703–4716 (2016).
30. J. Jeppesen, B. Kiens, Regulation and limitations to fatty acid oxidation during exercise. *J. Physiol.* **590**, 1059–1068 (2012).
31. J. A. Romijn *et al*., Regulation of endogenous fat and carbohydrate metabolism in relation to exercise intensity and duration. *Am. J. Physiol.* **265**, E380–E391 (1993).
32. J. R. Zierath, J. A. Hawley, Skeletal muscle fiber type: Influence on contractile and metabolic properties. *PLoS Biol.* **2**, e348 (2004).
33. S. Schiaffino, C. Reggiani, Fiber types in mammalian skeletal muscles. *Physiol. Rev.* **91**, 1447–1531 (2011).
34. S. Schiaffino, C. Reggiani, Molecular diversity of myofibrillar proteins: Gene regulation and functional significance. *Physiol. Rev.* **76**, 371–423 (1996).
35. Z.-X. Meng *et al*., Baf60c drives glycolytic metabolism in the muscle and improves systemic glucose homeostasis through Deptor-mediated Akt activation. *Nat. Med.* **19**, 640–645 (2013).
36. K. Y. Lee *et al*., Tbx15 controls skeletal muscle fibre-type determination and muscle metabolism. *Nat. Commun.* **6**, 8054 (2015).
37. Z. Arany *et al*., The transcriptional coactivator PGC-1β drives the formation of oxidative type IIX fibers in skeletal muscle. *Cell Metab.* **5**, 35–46 (2007).
38. D. M. Anderson *et al*., A micropeptide encoded by a putative long noncoding RNA regulates muscle performance. *Cell* **160**, 595–606 (2015).
39. C. Trollet, D. Scherman, P. Bigey, "Delivery of DNA into muscle for treating systemic diseases: Advantages and challenges" in *Electroporation Protocols: Preclinical and Clinical Gene Medicine*, S. Li, Ed. (Humana Press, Totowa, NJ, 2008), pp. 199–214.
40. J. D. Schertzer, D. R. Plant, G. S. Lynch, Optimizing plasmid-based gene transfer for investigating skeletal muscle structure and function. *Mol. Ther.* **13**, 795–803 (2006).
41. M. J. Molnar *et al*., Factors influencing the efficacy, longevity, and safety of electroporation-assisted plasmid-based gene transfer into mouse muscles. *Mol. Ther.* **10**, 447–455 (2004).
42. M. Gonzalez-Freire, R. de Cabo, S. A. Studenski, L. Ferrucci, The neuromuscular junction: Aging at the crossroad between nerves and muscle. *Front. Aging Neurosci.* **6**, 208 (2014).
43. K. I. Erickson *et al*., Brain-derived neurotrophic factor is associated with age-related decline in hippocampal volume. *J. Neurosci.* **30**, 5368–5375 (2010).
44. M. J. Webster, M. M. Herman, J. E. Kleinman, C. Shannon Weickert, BDNF and trkB mRNA expression in the hippocampus and temporal cortex during the human lifespan. *Gene Expr. Patterns* **6**, 941–951 (2006).
45. M. Silhol, V. Bonnichon, F. Rage, L. Tapia-Arancibia, Age-related changes in brain-derived neurotrophic factor and tyrosine kinase receptor isoforms in the hippocampus and hypothalamus in male rats. *Neuroscience* **132**, 613–624 (2005).
46. E. Palomer *et al*., Aging triggers a repressive Chromatin state at Bdnf promoters in hippocampal neurons. *Cell Rep.* **16**, 2889–2900 (2016).
47. F. Rage, M. Silhol, F. Binamé, S. Arancibia, L. Tapia-Arancibia, Effect of aging on the expression of BDNF and TrkB isoforms in rat pituitary. *Neurobiol. Aging* **28**, 1088–1098 (2007).
48. E. J. Huang, L. F. Reichardt, Neurotrophins: Roles in neuronal development and function. *Annu. Rev. Neurosci.* **24**, 677–736 (2001).
49. D. Merrick, T. Ting, L. K. Stadler, J. Smith, A role for Insulin-like growth factor 2 in specification of the fast skeletal muscle fibre. *BMC Dev. Biol.* **7**, 65 (2007).
50. A. C. Paul, N. Rosenthal, Different modes of hypertrophy in skeletal muscle fibers. *J. Cell Biol.* **156**, 751–760 (2002).
51. J. J. McCarthy, R. Srikuea, T. J. Kirby, C. A. Peterson, K. A. Esser, Inducible Cre transgenic mouse strain for skeletal muscle-specific gene targeting. *Skelet. Muscle* **2**, 8 (2012).
52. J. O. Holloszy, F. W. Booth, Biochemical adaptations to endurance exercise in muscle. *Annu. Rev. Physiol.* **38**, 273–291 (1976).
53. P. Klover, W. Chen, B.-M. Zhu, L. Hennighausen, Skeletal muscle growth and fiber composition in mice are regulated through the transcription factors STAT5a/b: Linking growth hormone to the androgen receptor. *FASEB J.* **23**, 3140–3148 (2009).
54. O. Agbulut, P. Noirez, F. Beaumont, G. Butler-Browne, Myosin heavy chain isoforms in postnatal muscle development of mice. *Biol. Cell* **95**, 399–406 (2003).
55. M. Nagano, H. Suzuki, Quantitative analyses of expression of GDNF and neurotrophins during postnatal development in rat skeletal muscles. *Neurosci. Res.* **45**, 391–399 (2003).
56. M. A. Grill *et al*., Tetracycline-inducible system for regulation of skeletal muscle-specific gene expression in transgenic mice. *Transgenic Res.* **12**, 33–43 (2003).
57. K. S. Krabbe *et al*., Brain-derived neurotrophic factor (BDNF) and type 2 diabetes. *Diabetologia* **50**, 431–438 (2007).
58. K. Marosi, M. P. Mattson, BDNF mediates adaptive brain and body responses to energetic challenges. *Trends Endocrinol. Metab.* **25**, 89–98 (2014).
59. M. Yamanaka *et al*., Brain-derived neurotrophic factor enhances glucose utilization in peripheral tissues of diabetic mice. *Diabetes Obes. Metab.* **9**, 59–64 (2007).
60. F. L. Mashili *et al*., Direct effects of FGF21 on glucose uptake in human skeletal muscle: Implications for type 2 diabetes and obesity. *Diabetes Metab. Res. Rev.* **27**, 286–297 (2011).
61. Y. Izumiya *et al*., FGF21 is an Akt-regulated myokine. *FEBS Lett.* **582**, 3805–3810 (2008).
62. J. Talbot, L. Maves, Skeletal muscle fiber type: Using insights from muscle developmental biology to dissect targets for susceptibility and resistance to muscle disease. *Wiley Interdiscip. Rev. Dev. Biol.* **5**, 518–534 (2016).
63. C. Handschin *et al*., PGC-1alpha regulates the neuromuscular junction program and ameliorates Duchenne muscular dystrophy. *Genes Dev.* **21**, 770–783 (2007).
64. V. Ljubicic *et al*., Chronic AMPK activation evokes the slow, oxidative myogenic program and triggers beneficial adaptations in mdx mouse skeletal muscle. *Hum. Mol. Genet.* **20**, 3478–3493 (2011).
65. S. Rauskolb *et al*., Global deprivation of brain-derived neurotrophic factor in the CNS reveals an area-specific requirement for dendritic growth. *J. Neurosci.* **30**, 1739–1749 (2010).